

Time-correlated forces and biological variability in cell motility

T. N. Azevedo¹, L. G. Rizzi^{1,*}

¹ Departamento de Física, Universidade Federal do Viçosa, CEP 36570-000, Viçosa, MG, Brazil.

Abstract

Cell motility is one of the most fundamental phenomena underlying biological processes that maintain living organisms alive. Here we introduce a simple model to describe the motility of cells which include not only time-correlated internal forces but also the biological variability which is inherent of the intra-cellular biochemical processes. Such model allow us to derive exact expressions for the mean-squared displacement and the effective time-dependent diffusion coefficient which are compared to numerical results obtained from non-markovian stochastic simulations. In addition, we show that the heterogeneity of persistence times lead to non-gaussian distributions which can be obtained analytically and that were validated by the numerical simulations. Our results indicate that such model might be used to describe the behaviour observed in experimental results obtained for isolated cells without external signaling.

Keywords:

cell motility, time-correlated forces, biological variability

1. Introduction

Active physical and chemical processes that affect the cellular behaviour play an important role in the homeostasis of almost all living organisms [1]. Cell motility, in particular, influences numerous fundamental biological processes, such as organogenesis (*i.e.*, cell aggregation and migration), wound healing, and tumor development [2, 3, 4].

In general, the stochastic dynamics of the cell movement exhibit properties that differ from the normal diffusive-like behaviour, which is often characterized by a mean-squared displacement that is given by

$$\langle \Delta r^2(\tau) \rangle \propto \tau^\alpha, \quad (1)$$

where the exponent α gives a measure whether their diffusive-like movement is anomalous (*i.e.*, when $\alpha \neq 1$) or not. As illustrated in Fig. 1, the experimental data extracted from Ref. [5] obtained from the motion of isolated cells (*i.e.*, without external signaling processes) provide an important evidence that cell's motility can be characterized by a superdiffusive behaviour at short times (with $\alpha > 1$) and by a normal diffusion regime (with $\alpha \approx 1$) at later times.

Although several models have been proposed to describe the different diffusive regimes observed in cell motility [6, 7, 8, 9, 10, 11], the persistent random walk (PRW) model is one of the most used models to describe experimental data (see, *e.g.*, refs. [5, 12, 13]). Besides its simplicity, such model captures the main feature of cell motility which is the time-correlation (*i.e.*, the persistence) of the random walk [2]. As shown in Fig. 1, the PRW model can be used to describe the experimental data for the MSD quite well. However, a closer look at the experimentally observed displacements and velocities distributions (see, *e.g.*, [14, 15, 16]) reveals that they might present non-gaussian tails which cannot be satisfactorily described by the usual PRW model. Interestingly, there are recent experimental evidence [2, 12, 17] suggesting that a possible source of the non-gaussianity of the distributions can be the inherent heterogeneities of intra-cellular processes that are present even in the absence of external signals.

Here we present a generalization of the PRW model which incorporates the cell-to-cell variability by considering that the persistence times λ of the internal processes which occur in each cell are distributed according to a distribution $\rho(\lambda)$, and show how it can alter the distributions of distances and velocities.

2. Time-correlated forces and stochastic simulations

Before introduce our model, we present some of the theoretical aspects related to the stochastic processes that characterize the PRW model as well as the numerical methodology which can be used to obtain its non-markovian dynamics.

2.1. Langevin approach

Consider that the cell movement can be effectively described by a simple force equation that is written as an overdamped Langevin-like equation as

$$\gamma \frac{d\vec{r}}{dt} = \vec{f}_s, \quad (2)$$

where γ is an effective adhesion (or friction) coefficient between the cell and the substrate, and \vec{f}_s is a stochastic intra-cellular (or internal) force [18]. Thus, the velocity of the cell, $\vec{v} = \gamma^{-1} \vec{f}_s$, can be also considered a stochastic variable. From the statistical point of view, we assume that it has the following properties: (i) $\langle \vec{v} \rangle = \vec{0} \mu\text{m}/\text{min}$ (*i.e.*, zero mean value); and, (ii) an autocorrelation that is given by

$$\langle \vec{v}(t) \cdot \vec{v}(t') \rangle = dv_0^2 A(t - t'), \quad (3)$$

where $v_0 \equiv f_s/\gamma$ is the velocity autocorrelation parameter, d is the dimension of the substrate, and $A(t - t')$ is an autocorrelation function that will be specified later. Here the average $\langle \dots \rangle$ is considered to be taken over an *ensemble* of independent cells. Accordingly, in order to incorporate the variability of those cells into our theoretical framework, we consider that the autocorrelation function can be written as

$$A(\tau) = \int_0^\infty \rho(\lambda) e^{-\tau/\lambda} d\lambda, \quad (4)$$

where $\tau = t - t'$, and $\rho(\lambda)$ is the distribution of persistence times λ .

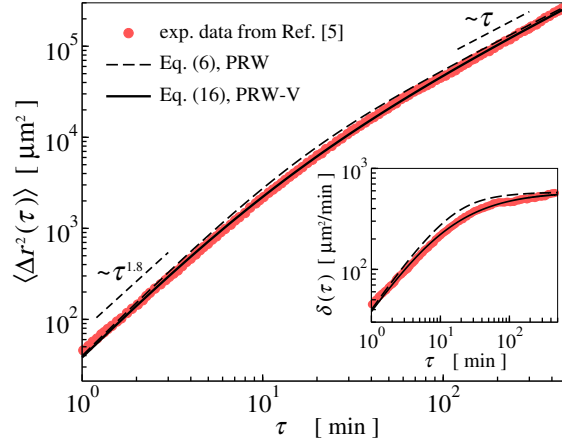


Figure 1: Comparison between the experimental data extracted from Ref. [5] (denoted by the filled red circles) and the theoretical results obtained from the usual persistent random walk (PRW) model, and the persistent random walk model with variability (PRW-V) introduced here. The main panel display the mean-squared displacement $\langle \Delta r^2(\tau) \rangle$, while the inset shows the ratio $\delta(\tau) = \langle \Delta r^2(\tau) \rangle / \tau$. Short dashed lines indicate the short-time superdiffusive, or ballistic, ($\alpha > 1$) and the normal diffusive behaviours ($\alpha \approx 1$) observed at later times. Long dashed and straight lines correspond to the PRW model, Eq. (6), and the PRW-V model, Eq. (16), respectively. Both models are described by the velocity autocorrelation parameter $v_0 = 4.57 \mu\text{m}/\text{min}$ and a persistence time $\tau_p = 7 \text{ min}$.

2.2. Persistent random walk (PRW) model

The PRW model can be easily retrieved from the above framework by considering that there is only a single persistence time τ_p which is common to all cells. This is done by choosing a delta distribution, *i.e.*, $\rho(\lambda) = \delta(\lambda - \tau_p)$, so that Eq. (4) yields $A(\tau) = e^{-\tau/\tau_p}$, and Eq. (3) leads to a velocity autocorrelation function that is also given by an exponential, *i.e.*, $\langle \vec{v}(\tau) \cdot \vec{v}(0) \rangle = dv_0^2 e^{-\tau/\tau_p}$. In addition, one can obtain the time-dependent diffusion coefficient $D(\tau)$ from the velocity autocorrelation function [19] which, for the PRW model, is given by the following expression

$$D(\tau) = d^{-1} \int_0^\tau \langle \vec{v}(t') \cdot \vec{v}(0) \rangle dt' = v_0^2 \tau_p \left[1 - \exp\left(-\frac{\tau}{\tau_p}\right) \right]. \quad (5)$$

Also, one can use the above result for $D(\tau)$ to obtain the MSD of the PRW model by integrating Eq. (5), that is,

$$\langle \Delta r^2(\tau) \rangle = (2d) \int_0^\tau D(t') dt' = 2dv_0^2 \tau_p \left[\tau - \tau_p (1 - e^{-\tau/\tau_p}) \right]. \quad (6)$$

The short-time behaviour ($\tau \ll \tau_p$) of the MSD can be easily obtained by expanding the exponential term in Eq. (6) up to second order, thus $\langle \Delta r^2(\tau) \rangle \approx dv_0^2 \tau^2$, which corresponds to the *ballistic regime*. On the other hand, for sufficiently long times, *i.e.*, $\tau \gg \tau_p$, one finds that the MSD should present a linear behaviour, that is, $\langle \Delta r^2(\tau) \rangle \approx 2dv_0^2 \tau_p (\tau - \tau_p)$, and that corresponds to the *normal diffusion regime*. We note that, although such limits are the same of those that can be observed for the experimentally obtained MSD presented in Fig. 1, expression (6) does not fit the data very well.

Although the difference between the experimental data and the results obtained from the PRW model can be already appreciated in the Fig. 1, the effects of the variability of the cells are better realized from the probability $p(x)$ of finding cells at a position x after a time τ given that they all started at the origin, $x = 0 \mu\text{m}$. If one consider that, despite of being non-markovian, the stochastic processes defined by Eq. (2) in the case of the PRW model are still gaussian processes, hence the position distribution should be given by

$$p(x) = \left(\frac{1}{2\pi \langle \Delta x^2(\tau) \rangle} \right)^{1/2} \exp \left[-\frac{x^2}{2 \langle \Delta x^2(\tau) \rangle} \right], \quad (7)$$

where $\langle \Delta x^2(\tau) \rangle = d^{-1} \langle \Delta r^2(\tau) \rangle$ with the MSD given by Eq. (6). Note that, by assuming that the random walk is isotropic, one has that the distribution $p(y)$ for the y -component should display the same functional form of the above equation with $\langle \Delta y^2(\tau) \rangle = d^{-1} \langle \Delta r^2(\tau) \rangle$.

In the following we illustrate how the above theoretical results for the PRW model can be obtained by considering numerical simulations that lead to non-markovian stochastic processes with a well-defined persistence time τ_p .

2.3. Non-markovian stochastic simulations

Numerically, the main quantity used to quantify the motility of the cells is their the mean-squared displacement (MSD), which is defined as

$$\langle \Delta r^2(\tau) \rangle = \langle [\vec{r}(\tau) - \vec{r}(0)]^2 \rangle, \quad (8)$$

where $\langle \dots \rangle$ denotes averages over the trajectories of N independent cells. In order to obtain the position of the cell $\vec{r}(t_k)$ at a time t_k one need to consider Eq. (2), which can be discretized and integrated according to the Euler's approximation scheme, that is, $\vec{r}(t_{k+1}) = \vec{r}(t_k) + (\vec{f}_s/\gamma)\Delta t$, where $t_{k+1} = t_k + \Delta t$ with $t_0 = 0$ min. By considering that the motion of the cells is restricted to a two-dimensional substrate (*i.e.*, $d = 2$), the implementation is similar to the usual Brownian dynamics algorithm discussed in Ref. [20], that is,

$$\vec{r}(t_{k+1}) = \vec{r}(t_k) + \sqrt{v_0^2 \Delta t} \left[\xi_x(t_k) \hat{x} + \xi_y(t_k) \hat{y} \right], \quad (9)$$

where we assume that the variables $\xi_x(t_k)$ and $\xi_y(t_k)$ are independent gaussian-distributed random variables with zero mean and variance equal to one. In order to obtain time-correlated velocities (or forces), we consider that the above defined random variables are generated by the following recursive scheme [21],

$$\xi_i(t_{k+1}) = \Lambda \xi_i(t_k) + \sqrt{1 - \Lambda^2} \xi'_i(t_k), \quad (10)$$

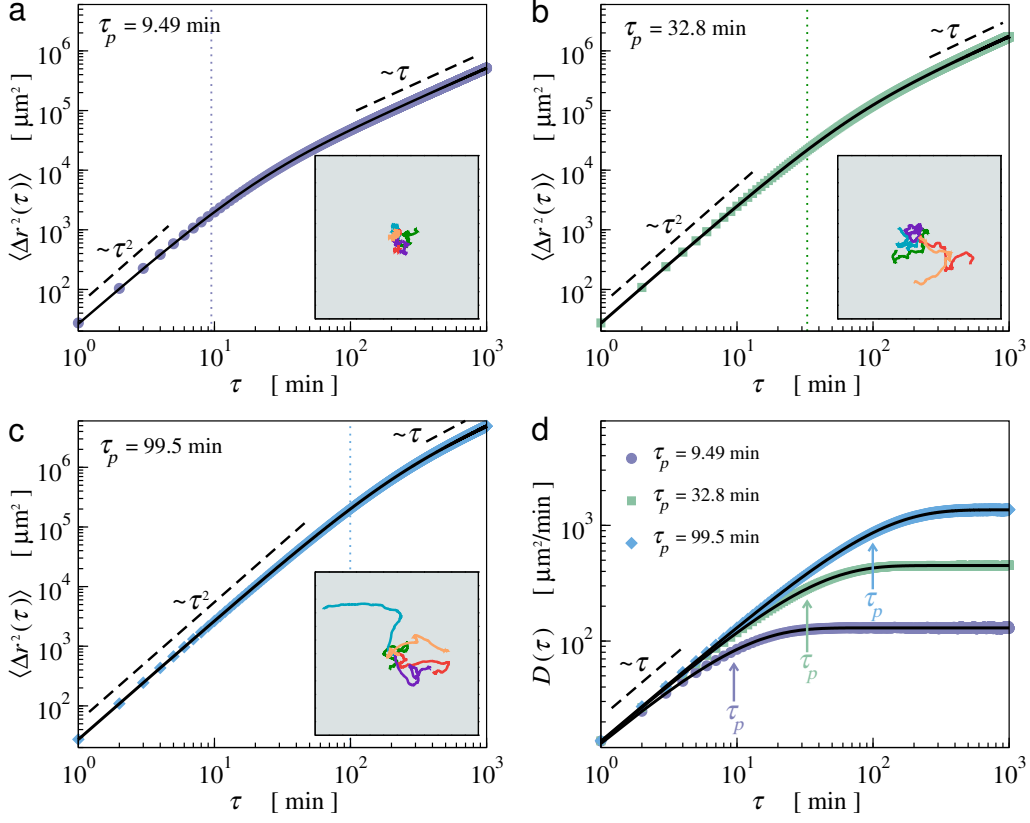


Figure 2: (a)-(c) Mean-squared displacement $\langle \Delta r^2(\tau) \rangle$ obtained for the PRW model defined with different autocorrelation times τ_p determined by the parameter Λ : (a) $\tau_p = 9.49$ min ($\Lambda = 0.9$), (b) $\tau_p = 32.8$ min ($\Lambda = 0.97$), and (c) $\tau_p = 99.5$ min ($\Lambda = 0.99$); (d) Time-dependent diffusion coefficient $D(\tau)$ for the three cases. Filled symbols correspond to the numerical data obtained through non-markovian stochastic simulations considering a two-dimensional substrate ($d = 2$), $v_0 = 3.7 \mu\text{m}/\text{min}$, $\Delta t = 1$ min, and $N = 10^6$ trajectories for each value of Λ . Straight black lines indicate the analytical results derived from the PRW model given by Eq. (5), $D(\tau)$, and Eq. (6), $\langle \Delta r^2(\tau) \rangle$, while dashed lines denote the observed ballistic (for $\tau \ll \tau_p$) and normal diffusive (for $\tau \gg \tau_p$) regimes. Insets: typical two-dimensional trajectories obtained for the different autocorrelation times τ_p .

where $\xi'_i(t_k)$ is a gaussian-distributed random variable with zero mean and variance equal to one, with $\xi'_i(t_0) = \xi_i(t_0)$, and Λ is a parameter in the range $0 < \Lambda < 1$. This procedure lead to random varying velocities with an autocorrelation $A(t_k) = \langle \xi'_i(t_k) \cdot \xi'_i(0) \rangle \approx e^{-t_k/\tau_p}$ that is determined by a persistence (*i.e.*, characteristic autocorrelation) time τ_p , just like in the PRW model. As discussed in Ref. [21], the value of τ_p can be related to the parameter Λ as

$$\tau_p = -\frac{1}{\ln \Lambda} . \quad (11)$$

Importantly, although this procedure ensures that the internal forces of the cell present an exponential time correlation, it keeps their statistical properties, *i.e.*, the stochastic process will be still a gaussian process with zero mean so that the distribution $p(x)$ will be given by Eq. (7) at any time τ (data not shown).

Figure 2 shows a comparison between the MSDs obtained from the above numerical scheme for different persistence times τ_p and the theoretical results expected from the PRW model. As one can see in the inset panels, the trajectories are more localized for shorter autocorrelation times τ_p . Higher values of the persistence times ($\tau_p = 99.5$ min) lead to more spread trajectories. Such diffusive-like behaviour, which is typical of the PRW model, can be probed by a more sensitive analysis that considers the time-dependent diffusion coefficient, which can be evaluated numerically from the MSD as

$$D(\tau) = \frac{1}{2d} \frac{d\langle \Delta r^2(\tau) \rangle}{d\tau} . \quad (12)$$

As displayed in Fig. 2(d), the time-dependent diffusion coefficient $D(\tau)$ indicate that there is a clear separation between the ballistic regime at short times, where $D(\tau) \approx v_0^2 \tau$, and the normal diffusive-like behaviour at $\tau \gg \tau_p$, where the diffusion coefficient is constant, *i.e.*, $D(\tau) \approx v_0^2 \tau_p$, just as expected from Eq. (5).

3. Persistent random walk with variability (PRW-V)

Now, in order to incorporate the cell-to-cell variability into our theoretical framework, we assume that the distribution of persistence times is given by a generalized inverse gamma distribution [22], that is,

$$\rho(\lambda) = \frac{1}{\tau_p \Gamma(b)} \left(\frac{\tau_p}{\lambda} \right)^{b+1} \exp\left(-\frac{\tau_p}{\lambda}\right), \quad (13)$$

where $\Gamma(b)$ is the usual gamma function. Here, it is convenient to consider the change of variables¹ $\theta = \tau_p/\lambda$, so that $\rho(\theta) = \theta^{b-1} e^{-\theta}/\Gamma(b)$ and $e^{-\tau/\lambda} = e^{-\theta(\tau/\tau_p)}$ in Eq. (4). Thus, the distribution $\rho(\theta)$ is a simple gamma distribution [22] that can be used to evaluate both the mean persistence time, $\bar{\lambda} = \tau_p/(b-1)$, and the autocorrelation function, which is given by $A(\tau) = [1 + (\tau/\tau_p)]^{-b}$. Importantly, the expression (13) is defined as a generic distribution that could be used to describe the experimental data, *e.g.*, the distribution of dwell times in Ref. [17]. Although several values can be attributed to the exponent b , here we consider that $b = 2$ in order to have the mean value $\bar{\lambda}$ consistent with a given persistence time, that is, $\bar{\lambda} = \tau_p$. Hence, Eq. (3) leads to a velocity autocorrelation function given by

$$\langle \vec{v}(\tau) \cdot \vec{v}(0) \rangle = dv_0^2 \left[1 + \left(\frac{\tau}{\tau_p} \right) \right]^{-2}. \quad (14)$$

As a result, the time-dependent diffusion coefficient $D(\tau)$ and the MSD $\langle \Delta r^2(\tau) \rangle$ of the PRW-V model can be obtained by integration of the above expression (see Section 2.2), which yields, respectively,

$$D(\tau) = v_0^2 \tau_p \left\{ 1 - \left[1 + \left(\frac{\tau}{\tau_p} \right) \right]^{-1} \right\}, \quad (15)$$

and

$$\langle \Delta r^2(\tau) \rangle = 2dv_0^2 \tau_p \left\{ \tau - \tau_p \ln \left[1 + \left(\frac{\tau}{\tau_p} \right) \right] \right\}. \quad (16)$$

Interestingly, the short and the later time behaviours of the time-dependent diffusion coefficient, Eq. (15), are similar to the results obtained from the PRW model in Section 2.2, that is, $D(\tau) \approx v_0^2 \tau$ for $\tau \ll \tau_p$, and $D(\tau) \approx v_0^2 \tau_p$ for $\tau \gg \tau_p$. However, although the short time limit of Eq. (16) is similar to the MSD of the PRW model, *i.e.*, $\langle \Delta r^2(\tau) \rangle \approx dv_0^2 \tau^2$, the presence of the logarithm leads to a slightly different behaviour for later times.

In Fig. 3 we include results for the PRW-V model and its comparison to the usual PRW model. The numerical simulations were carried out just as described in Section 2.3, however, the N trajectories were obtained by considering different values for Λ in Eq. (11). In particular, we consider that the distribution of persistence times, $\lambda = -1/\ln \Lambda$, follows Eq. (13) with $b = 2$ and $\bar{\lambda} = \tau_p = 9.49$ min, as shown in Fig. 3(a). Accordingly, the MSD presented in Fig. 3(c) shows a behaviour that is similar to the experimental results presented in Fig. 1. Although the difference between the PRW and PRW-V seems to be small for the MSD and the ratio $\delta(\tau)$, it is clear from the time-dependent diffusion coefficient $D(\tau)$ in Fig. 3(b) that the numerical results obtained from simulations with variability are better described by the PRW-V model.

Next we show that the differences between the usual PRW and the PRW-V models are significantly greater when one looks to the position and velocity distributions at later times.

¹Note that this change of variables should include the Jacobian factor, that is, $\rho(\theta) = \rho(\lambda)|_{\lambda=\tau_p/\theta} (\partial\lambda/\partial\theta)$.

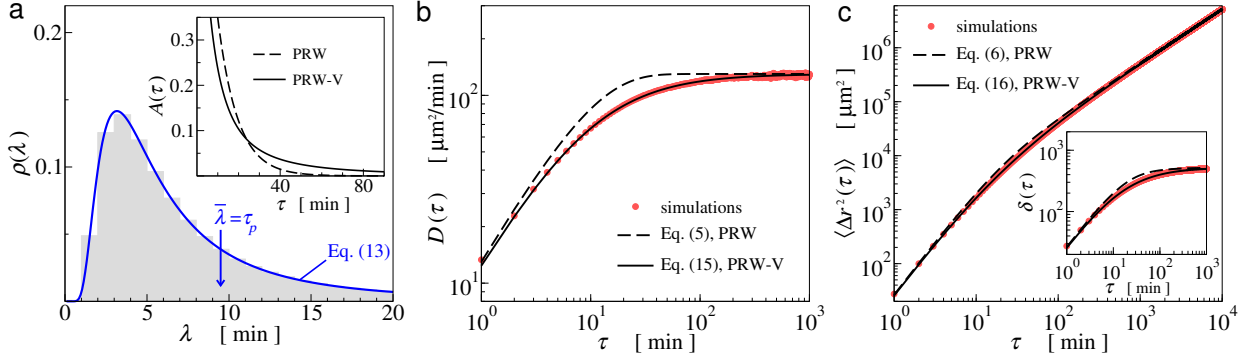


Figure 3: Numerical and theoretical results obtained for the PRW-V model considering that the persistence times are randomly distributed according to Eq. (13) with $\bar{\lambda} = \tau_p = 9.49$ min (*i.e.*, $b = 2$), $v_0 = 3.7 \mu\text{m}/\text{min}$, $\Delta t = 1$ min, and $N = 10^6$ independent two-dimensional ($d = 2$) trajectories. (a) Numerically obtained histograms (grey bars) and the expected analytical distribution (straight blue line) of persistence times $\rho(\lambda)$. Inset panel displays a comparison between the autocorrelation functions $A(\tau)$ of the PRW and the PRW-V models. (b) Time-dependent diffusion coefficient $D(\tau)$. (c) Mean-squared displacement $\langle \Delta r^2(\tau) \rangle$ and the ratio $\delta(\tau) = \langle \Delta r^2(\tau) \rangle / \tau$ (inset panel).

4. Distributions for the PRW-V model

Besides the position distribution $p(x)$, an often computed quantity from experiments is the distribution $p(v_x)$, which is related to the components of the velocity of the cells that can be defined as $\vec{v}_\tau = [\vec{r}(\tau+t_0) - \vec{r}(t_0)]/\tau = \vec{r}(\tau)/\tau$. If the stochastic processes that lead to the motion of the cells are gaussian processes, the distributions of the components of \vec{r} are given by Eq. (7), thus the distributions of the components v_x of the velocities \vec{v}_τ will be also given by gaussian distributions. Thus, for the PRW model, in particular, the distribution $p(v_x)$ can be evaluated directly from Eq. (7) and is given by

$$p(v_x) = \left(\frac{1}{2\pi \langle \Delta v_x^2(\tau) \rangle} \right)^{1/2} \exp \left[-\frac{v_x^2}{2 \langle \Delta v_x^2(\tau) \rangle} \right], \quad (17)$$

where $\langle \Delta v_x^2(\tau) \rangle = \langle \Delta x^2(\tau) \rangle / \tau^2$. As shown in Figs. 4(a)-(h), the histograms evaluated from the numerical data (filled symbols) obtained for the PRW-V model display a clear departure from the corresponding gaussian distributions, *i.e.*, Eqs. (7) and (17), of the usual PRW model.

In order to obtain analytical expressions for the distributions $p(x)$ and $p(v_x)$ for the PRW-V model, one can consider that the gaussian distributions of the PRW model given by Eqs. (7) and (17) are equivalent to conditional probabilities, that is, $p(z|\lambda)$, since their variance $\langle \Delta z_\lambda^2(\tau) \rangle$ depend on the persistence times λ (here z could denote either the component of the position x or of the velocity v_x). In fact, those probabilities can be also written in terms of $\theta = \tau_p/\lambda$, that is, $p(z|\theta) = 1 / (2\pi \langle \Delta z_\theta^2(\tau) \rangle)^{1/2} \exp[-z^2 / 2 \langle \Delta z_\theta^2(\tau) \rangle]$. Unfortunately, the expressions for the variances, *i.e.*, $\langle \Delta x_\theta^2(\tau) \rangle$ and $\langle \Delta v_x^2(\tau) \rangle$, may lead to non-trivial joint distributions $p(z, \theta) = p(z|\theta) \rho(\theta)$ that cannot be easily marginalized [23]. Even so, at later times, $\tau \gg \tau_p$, the variances can be approximated by $\langle \Delta z_\theta^2(\tau) \rangle \approx \sigma_z^2 / \theta$, with $\sigma_x^2 \approx 2v_0^2 \tau_p \tau$ and $\sigma_{v_x}^2 = \sigma_x^2 / \tau^2 \approx 2v_0^2 \tau_p / \tau$. Thus, one can use $p(z|\theta)$ together with the prior distribution $\rho(\theta)$ given in Section 3 to evaluate the distributions of position and velocity of the PRW-V at later times, *i.e.*, $\tau \gg \tau_p$, as

$$p(z) = \int_0^\infty p(z|\theta) \rho(\theta) d\theta \approx \frac{3}{4 \sqrt{2\sigma_z^2}} \left(1 + \frac{z^2}{2\sigma_z^2} \right)^{-5/2}. \quad (18)$$

where z can be either the component of the position x or of the velocity v_x , and σ_z^2 denote estimates for the corresponding variances, *i.e.*, $\langle \Delta x^2(\tau) \rangle$ and $\langle \Delta v_x^2(\tau) \rangle$. Indeed, by considering $v_0 = 3.7 \mu\text{m}/\text{min}$, $\tau_p = 9.49$ min, and $\tau = 2000$ min, one gets $\sigma_x^2 \approx 2v_0^2 \tau_p \tau \approx 5.2 \times 10^5 \mu\text{m}^2$, so that the agreement of the above expression, Eq. (18), for $p(x)$ and the numerical data presented for the PRW-V in Fig. 4(h) is remarkable. A good agreement is also observed between the numerical results and the $p(v_x)$ given by Eq. (18) with $\sigma_{v_x}^2 = \sigma_x^2 / \tau^2 \approx 2v_0^2 \tau_p / \tau \approx 0.13 \mu\text{m}^2/\text{min}^2$ in Fig. 4(d), *i.e.*, at later times.

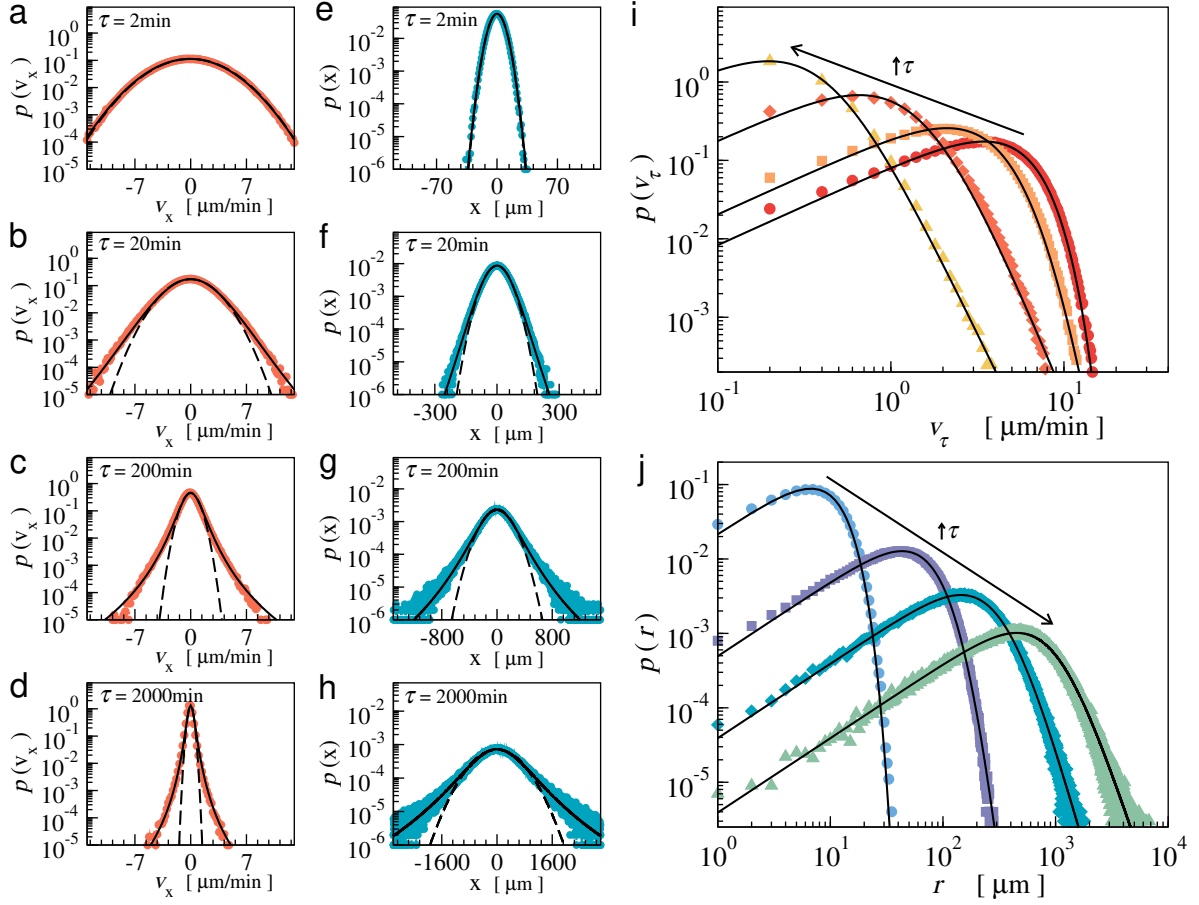


Figure 4: Distributions of velocities and displacements obtained for the PRW-V defined by autocorrelation times determined by the distribution $\rho(\lambda)$ given by Eq. (13) with $\bar{\lambda} = \tau_p = 9.49$ min at different times τ . Filled symbols correspond to the histograms evaluated from the numerical data obtained by Brownian dynamics simulations with $v_0 = 3.7$ $\mu\text{m}/\text{min}$, $\Delta t = 1$ min, and $N = 10^6$ independent trajectories in a two-dimensional substrate ($d = 2$). Straight black lines in panels (a)-(h) correspond to component distributions $p(z)$ given by Eq. (19), while the distributions $w(r)$ and $w(v_\tau)$ in (i) and (j) are given by expression (22). Dashed black lines in panels (a)-(h) correspond to gaussian distributions, e.g., Eqs. (7) and (17). At later times, $\tau \gg \tau_p$, the distributions are well described by the approximated expressions given by Eqs. (18) and (21).

It is worth noting that the expression (18) is a particular case of a more general distribution called Pearson (type VII) distribution [22], which is given by

$$p(z) = \frac{1}{|s| B(m - 1/2, 1/2)} \left(1 + \frac{z^2}{s^2}\right)^{-m} \quad (19)$$

where $B(l, c) = \int_0^1 u^{l-1} (1-u)^{c-1} du$ is the so-called beta function. Interestingly, one can assume that $s^2 = (2m - 3)\sigma_z^2$ (for $m > 3/2$), so that $p(z)$ yields exactly the same distribution given by Eq. (18) at later times, i.e., with $m = 5/2$, $B(2, 1/2) = 4/3$, and $s^2 = 2\sigma_z^2$. In fact, as shown in Fig. 4(a)-(h), different values of the exponent m can be used to interpolate between the later times ($\tau \gg \tau_p$), where the distributions $p(z)$ are given by Eq. (18) with $m = 5/2$, and short times ($\tau \ll \tau_p$), where the exponent m assumes large values and the distributions $p(z)$ given by Eq. (19) correspond to gaussian distributions² with variance σ_z^2 .

²One can verify that by considering the relationship $B(l, c) = \Gamma(l)\Gamma(c)/\Gamma(l+c)$, and replace $B(m - 1/2, 1/2)$ and $s = \sqrt{2(m - 3/2)\sigma_z^2}$ into Eq. (19), so that the limit of $m \rightarrow \infty$ of the Pearson distribution yields the prefactor $1/\sqrt{2\pi\sigma_z^2}$ times a z -dependent exponential, i.e., $\exp(-z^2/2\sigma_z^2)$, just like the gaussian distributions given by Eqs. (7) and (17).

Next, we turn our attention to the distributions of distances, $r = \sqrt{x^2 + y^2}$, and velocities, $v_\tau = r/\tau$, as they are commonly evaluated by the experimentalists. For the two-dimensional ($d = 2$) PRW model one have that those distributions are given by the Rayleigh distributions [24], that is,

$$w(r) = \frac{2r}{\langle \Delta r^2(\tau) \rangle} \exp \left[-\frac{r^2}{\langle \Delta r^2(\tau) \rangle} \right] \quad \text{and} \quad w(v_\tau) = \frac{2v_\tau}{\langle \Delta v_\tau^2(\tau) \rangle} \exp \left[-\frac{v_\tau^2}{\langle \Delta v_\tau^2(\tau) \rangle} \right], \quad (20)$$

where $\langle \Delta v_\tau^2(\tau) \rangle = \langle \Delta r^2(\tau) \rangle / \tau^2$, with the MSD of the PRW model $\langle \Delta r^2(\tau) \rangle$ given by Eq. (6). The corresponding distributions for the PRW-V can be obtained by considering a similar approach that lead to Eq. (18), so that, at least for the limiting case where $\tau \gg \tau_p$, one have that

$$w(z) = \int_0^\infty w(z|\theta) \rho(\theta) d\theta \approx \frac{4z}{\Delta_z^2} \left(1 + \frac{z^2}{\Delta_z^2} \right)^{-3}. \quad (21)$$

where z can be either the distance r , so that $\Delta_r^2 \approx 2dv_0^2\tau\tau_p$, or the velocity v_τ , with $\Delta_{v_\tau}^2 = \Delta_r^2/\tau^2 \approx 2dv_0^2\tau_p/\tau$. Indeed, as shown in Figs. 4(i) and (j), the above expression is very accurate to describe the numerical data at later times, *i.e.*, $\tau = 2000$ min. Interestingly, Eq. (21) can be considered a limiting case of the Burr (type XII) distribution [22], which is given by

$$w(z) = \frac{2nz}{s^2} \left(1 + \frac{z^2}{s^2} \right)^{-(n+1)}, \quad (22)$$

where one can assume the specialization $s^2 = (n-1)\Delta_z^2$ (for $n > 1$). Accordingly, such distribution approaches the Rayleigh distributions, Eqs. (20), for large values of n , and it is equal to Eq. (21) if $n = 2$, which is the limit for later times. As indicated by the numerical data presented in Figs. 4(i) and 4(j), the above expression can be used to describe the numerical data obtained for the PRW-V remarkably well. Since both expressions (18) and (21) were obtained from the same distribution of persistence times $\rho(\lambda)$, one can expect that the exponents defined in the distributions (19) and (22) should be related as $n = m - 1/2$. Indeed, that relationship can be verified to be generally valid for all the data displayed in Fig. 4. Gaussian-like distributions, or equivalently, Rayleigh-like distributions (with $n \approx 26$), are observed only for short times, *i.e.*, $\tau = 2$ min. Finally, it is worth mentioning that Eq. (22) is similar to the q -Weibull distribution that was used to fit the experimental data obtained for the diffusive behaviour of non-isolated cells [25]. A comparison between the two expressions lead to $q = (n+2)/(n+1) \approx 1.33$ at later times (*i.e.*, $n = 2$ for $\tau \gg \tau_p$), which is close to the values found in Ref. [25], even though here we are considering only isolated cells.

5. Concluding remarks

In this work we introduce novel computational and theoretical approaches in order to explore the effect of time-correlated forces in the diffusion of active specimens and apply them to describe cell motility. By considering non-markovian stochastic simulations that display exponential autocorrelations with well-determined persistence times, we were able to generate persistent random walks that incorporate the biological variability that is inherent to the processes that occur in the intra-cellular media. Our numerical and analytical results suggest that the heterogeneity of persistence times can be directly related to the non-gaussianity of the distributions observed in experiments. Although we have considered a specific distribution $\rho(\lambda)$, depending on the cell line it might be interesting to consider slightly different values for the exponent b in Eq. (13). Importantly, here we have choose $b = 2$ in order to set $\bar{\lambda} = \tau_p$, but reliable experimental estimates for that value might be inferred from the velocity autocorrelation function, Eq. (14), since $A(\tau) = [1 + (\tau/\tau_p)]^{-b}$ for the PRW-V model. Also, we believe that, with the ideas developed here, the generalization of the distributions $w(r)$ and $w(v_\tau)$ to three-dimensional substrates should be straightforward.

Finally, it is worth mentioning that subdiffusive motility, *i.e.*, with the MSD characterized by Eq. (1) with $\alpha < 1$, can be considered within the non-markovian stochastic simulations of the PRW-V model simply by adding a hookean-like force, *i.e.*, $\vec{F}(\vec{r}) = -\kappa\vec{r}$, to the right hand side of Eq. (2). We think that could be an interesting way to extend the present framework to cases where the cells are moving in confined and/or crowded environments.

Acknowledgements

The authors acknowledge the useful discussions with Professor Marcelo Lobato Martins and the financial support of the Brazilian agencies, CAPES (code 001) for the Scholarship, CNPq (Grants N^o 306302/2018-7 and N^o 426570/2018-9), and FAPEMIG (Process APQ-02783-18).

References

References

- [1] F. Höfling, T. Franosch, Anomalous transport in the crowded world of biological cells, *Rep. Prog. Phys.* 76 (2013) 046602.
- [2] R. Petrie, A. Doyle, K. Yamada, Random versus directionally persistent cell migration, *Nat. Rev. Mol. Cell. Biol.* 10 (2009) 538.
- [3] C. T. Mierke, D. Rösel, B. Fabry, J. Brábek, Contractile forces in tumor cell migration, *European Journal of Cell Biology* 87 (2008) 669.
- [4] M. C. Weiger, V. Vedham, C. H. Stuelten, K. Shou, M. Herrera, M. Sato, W. Losert, C. A. Parent, Real-time motion analysis reveals cell directionality as an indicator of breast cancer progression, *Plos ONE* 8 (2013) e58859.
- [5] L. Li, S. F. Nørrelykke, E. C. Cox, Persistent cell motion in the absence of external signals: A search strategy for eukaryotic cells, *PLoS ONE* 3 (2008) e2093.
- [6] D. Selmecezi, S. Mosler, P. H. Hagedorn, N. B. Larsen, H. Flyvbjerg, Cell motility as persistent random motion: Theories from experiments, *Biophys. J.* 89 (2005) 912.
- [7] F. Peruani, L. G. Morelli, Self-propelled particles with fluctuating speed and direction of motion in two dimensions, *Phys. Rev. Lett.* 99 (2007) 010602.
- [8] P. Dieterich, R. Klages, R. Preuss, A. Schwab, Anomalous dynamics of cell migration, *Proc. Natl. Acad. Sci. USA* 105 (2008) 459.
- [9] D. Campos, V. Méndez, I. Llopis, Persistent random motion: Uncovering cell migration dynamics, *J. Theor. Biol.* 267 (2010) 526.
- [10] F. Safaeifard, S. P. Shariatpanahi, B. Goliaei, A survey on random walk-based stochastic modeling in eukaryotic cell migration with emphasis on its application in cancer, *Multidisciplinary Cancer Investigation* 2 (2018) 1.
- [11] G. L. Thomas, I. Fortuna, G. C. Perrone, J. A. Glazier, J. M. Belmonte, R. M. de Almeida, Parameterizing cell movement when the instantaneous cell migration velocity is ill-defined, *Physica A* 550 (2020) 124493.
- [12] P.-H. Wu, A. Giri, S. X. Sun, D. Wirtz, Three-dimensional cell migration does not follow a random walk, *Proc. Natl. Acad. Sci. USA* 111 (2014) 3949.
- [13] I. D. Luzhansky, A. D. Schwartz, J. D. Cohen, J. P. MacMunn, L. E. Barney, L. E. Jansen, S. R. Peyton, Anomalous diffusing and persistently migrating cells in 2D and 3D culture environments, *APL Bioeng.* 2 (2018) 026112.
- [14] H. Takagi, M. J. Sato, T. Yanagida, M. Ueda, Functional analysis of spontaneous cell movement under different physiological conditions, *PLoS ONE* 3 (2008) e2648.
- [15] H. Ebata, A. Yamamoto, Y. Tsuji, S. Sasaki, K. Moriyama, T. Kuboki, S. Kidoaki, Persistent random deformation model of cells crawling on a gel surface, *Sci. Rep.* 8 (2018) 5153.
- [16] S. Huda, B. Weigelin, K. Wolf, K. V. Tretiakov, K. Polev, G. Wilk, M. Iwasa, F. S. Emami, J. W. Narojczyk, M. Banaszak, S. Soh, D. Pilans, A. Vahid, M. Makurath, P. Friedl, G. G. Borisy, K. Kandere-Grzybowska, B. A. Grzybowski, Lévy-like movement patterns of metastatic cancer cells revealed in microfabricated systems and implicated in vivo, *Nat. Commun.* 9 (2018) 4539.
- [17] D. B. Brückner, A. Fink, J. O. Rädler, C. P. Broedersz, Disentangling the behavioural variability of confined cell migration, *J. R. Soc. Interface* 17 17 (2020) 20190689.
- [18] J. R. Lange, B. Fabry, Cell and tissue mechanics in cell migration, *Experimental Cell Research* 319 (2013) 2418.
- [19] M. Doi, *Soft Matter Physics*, 1st Edition, Oxford University Press, 2013.
- [20] D. Gillespie, Fluctuation and dissipation in brownian motion, *Am. J. Phys.* 61 (1993) 1077.
- [21] W. Janke, *Introduction to Simulation Techniques*, Springer Berlin Heidelberg, Berlin, Heidelberg, 2007, pp. 207–260.
- [22] G. E. Crooks, *Field Guide to Continuous Probability Distributions*, 2019.
- [23] E. T. Jaynes, *Marginalization and prior probabilities*, *Studies in Bayesian Statistics* (1978).
- [24] J. W. Strutt(Rayleigh), The problem of the random walk, *Nature* 72 (1905) 318.
- [25] T. S. V. Podesta, T. V. Rosembach, A. A. dos Santos, M. L. Martins, Anomalous diffusion and q -weibull velocity distributions in epithelial cell migration, *PLoS ONE* 12(7): 12 (2017) 7.